Rev Environ Sci Biotechnol (2017) 16:625–645
DOI 10.1007/s11157-017-9443-0

REVIEW PAPER

# Modeling the temperature effect on the specific growth rate of phytoplankton: a review

**Ghjuvan Micaelu Grimaud · Francis Mairet · Antoine Sciandra · Olivier Bernard**

Published online: 9 September 2017


**Abstract** Phytoplankton are key components of ecosystems. Their growth is deeply influenced by temperature. In a context of global change, it is important to precisely estimate the impact of temperature on these organisms at different spatial and temporal scales. Here, we review the existing deterministic models used to represent the effect of temperature on microbial growth that can be applied to phytoplankton. We first describe and provide a brief mathematical analysis of the models used in constant conditions to reproduce the thermal growth curve. We present the mechanistic assumptions concerning the effect of temperature on the cell growth and mortality, and discuss their limits. The coupling effect of temperature and other environmental factors such as light are then shown. Finally, we introduce the models taking into account the acclimation needed to thrive with temperature variations. The need for new thermal models, coupled with experimental validation, is argued.

**Keywords** Temperature growth models · Thermal growth curve · Protein thermal stability · Phytoplankton · Microalgae · Cyanobacteria

**Electronic supplementary material** The online version of this article (doi:10.1007/s11157-017-9443-0) contains supplementary material, which is available to authorized users.

G. M. Grimaud (✉) · F. Mairet · O. Bernard
BIOCORE-INRIA, BP93, 06902 Sophia-Antipolis Cedex, France
e-mail: grimaudg@msu.edu

A. Sciandra
UMR 7093, LOV, Observatoire Oceanologique, CNRS, UPMC Univ Paris 06, 06234 Villefranche, France

## 1 Introduction

Recent estimations predict a global temperature increase of 1–5 °C by the year 2100 (Rogelj et al. 2012). In this context, the microbial communities, either terrestrial or aquatic, are expected to be deeply impacted (Frey et al. 2013; Vezzulli et al. 2012; Thomas et al. 2012). Unicellular organisms are ectotherms and cannot regulate their temperature. They are thus particularly sensitive to temperature, which controls cellular metabolism by affecting enzymatic activity (Privalov 1979; Kingsolver 2009) and stability (Privalov 1979; Danson et al. 1996; Eijsink et al. 2005). Microorganisms play a key ecological role since they are involved in most of the biogeochemical fluxes (Paul 2014; Fuhrman et al. 2015). Especially, the autotrophic unicellular organisms (i.e. phytoplankton) are the basis of trophic chains in the majority of ecological systems (Field et al. 1998). Modeling the effect of temperature on phytoplankton physiology and cellular metabolism is thus crucial for better predicting ecosystems evolution in a changing environment.

In balanced growth conditions, the net growth rate of every microorganism as a function of temperature is

an asymmetric curve (see Fig. 1) called the thermal growth curve or the thermal reaction norm (Kingsolver 2009). The cardinal temperatures corresponding to the boundaries of thermal tolerance are defined as the minimal ($T_{min}$) and maximal ($T_{max}$) temperatures for growth. The temperature for which growth is maximal is called the optimal temperature ($T_{opt}$). The growth rate obtained at $T_{opt}$ is the maximal growth rate $\mu_{opt}$, whenever all the other factors affecting growth are non-limiting. The thermal range on which a given species can thrive is the thermal niche width (i.e. $T_{max} - T_{min}$). The asymmetry of the growth curve results from differential effects on physiology at low (under $T_{opt}$) and high (above $T_{opt}$) temperatures. At low temperatures the rate of every enzymatic biochemical reactions are affected. At high temperatures, structure and stability of some cellular components, such as key enzymes or membrane compounds (mainly lipids or proteins) are denatured. The consequences on cell metabolism and integrity leads to an increase in mortality (Serra-Maia et al. 2016). These deleterious effects depend on the time spent at high temperature, while the 'thermal dose' represents the temperature damages (Holcomb et al. 1999). The combined effects on metabolism, cell regulation mechanisms and cell integrity give the thermal growth curve (Corkrey 2014; Ghosh et al. 2016). While most of these underlying mechanisms have not been fully elucidated, several authors have proposed macroscopic models to represent this thermal growth curve. These simple models account for a minimum number of variables and do not provide a detailed mechanistic description of the involved biochemical underlying phenomena.

The aim of this study is to summarize the existing deterministic temperature growth models that can be used for phytoplankton, and to clarify the assumptions on the considered physiological processes. Firstly, models in non-limited and balanced growth conditions (i.e. when all the cell variables grow at the same constant rate over time) are described. The key hypotheses are explored through the review of growth models as well as the representation of the effect of temperature on cell mortality. Secondly, the coupling effect of temperature and other environmental factors such as light is addressed. Thirdly, a guideline is proposed to choose a model depending on the modelling purposes. Then, we present models taking into account temperature variations. The challenges to design a new generation of thermal models are finally discussed.

## 2 Modeling the specific growth rate of unicellular organisms as a function of temperature: the thermal growth curve

In this section, we detail the existing models dedicated to the effect of temperature on the specific growth rate of microorganisms in non-limiting conditions (see Tables 1, 2 for a summary). As discussed latter on, the specific growth rate concept (i.e. biomass increase per unit of time per unit of biomass) is highly dependent on the biomass descriptor.

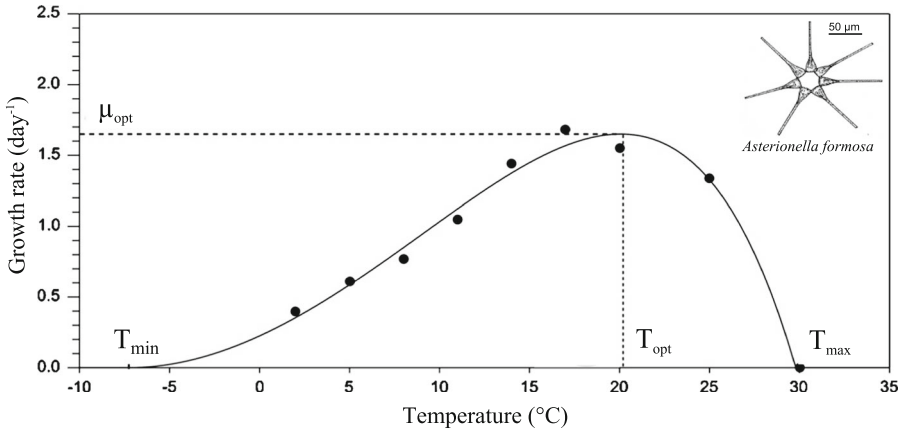


**Fig. 1** Thermal growth curve of the microalgae species *Astrionella formosa* [redrawn from Bernard and Rémond (2012)]

**Table 1** Synthesis of the main models for growth rate as a function of temperature (see also Sect. 3.1)

| Model | Type | # Parameters | Validation (data sets) | Cardinal temperatures | Mortality |
|---|---|---|---|---|---|
| Empirical models | | | | | |
| Square-root | E | 4 | 29, Bacteria (Ratkowksy et al. 1983) | $T_{min}$ and $T_{max}$ are explicit $T_{opt}$ is found by numerical optimization | No |
| CTMI | E | 4 | 47, Bacteria and yeast (Rosso et al. 1993) | Explicit | No |
| Blanchard | E | 4 | 2, Benthic phytoplankton (Blanchard et al. 1996) | $T_{opt}$ and $T_{max}$ are explicit $T_{min}$ is not defined | No |
| Bernard and Rémond | E | 4 | 15, Phytoplankton (Bernard and Rémond 2012) | Explicit | No |
| Eppley–Norberg | SE | 4 | 5, Phytoplankton (Norberg 2004) | $T_{opt} = \frac{bz - 1 + \sqrt{(w/2)^2 b^2 + 1}}{b}$ $\text{abs}(T_{max} - T_{min}) = w$ | No |
| Semi-empirical models | | | | | |
| Arrhenius equation | SE | 2 | – | Not defined | No |
| General mechanistic models | | | | | |
| Master reaction (for eq. 19) | M | 4 | 1, Normalized, bacteria (Johnson and Lewin 1946) and then yeast (Uden 1985) | $T_{opt} = \frac{\Delta H^{\ddagger}/R}{\ln\left(\frac{-\Delta H^{\ddagger} e^{\Delta S} - \Delta H e^{\Delta S}}{\Delta H}\right)}$ $T_{min}$ and $T_{max}$ are not defined | Yes (implicit) |
| Hinshelwood | M | 4 | No | $T_{opt} = \frac{E_1 - E_2}{R\ln\left(\frac{A_1 E_1}{A_2 E_2}\right)}$ $T_{max} = \frac{E_1 - E_2}{R\ln\left(\frac{A_1}{A_2}\right)}$ $T_{min} = T_{opt}\left(\frac{-E_1/\gamma}{T_{opt} - E_2/\gamma}\right)$ with $\gamma = R\ln(A_2/A_1\epsilon(E_2 - E_1)/E_1)$ | Yes (explicit) |
| DEB theory | M | 6 | No | $T_{min}$ and $T_{max}$ are not defined $T_{opt}$ is found numerically | Yes (implicit) |
| Protein-stability based models | | | | | |
| Modified Master reaction | M | 4 | 230, Normalized, all microorganisms (Corkrey 2014) | $T_{opt} = \frac{\Delta C_p T_0 + \Delta H}{\Delta C_p + R}$ $T_{min}$ and $T_{max}$ are not defined | Yes (implicit) |
| Proteome based | M | 2 | 12, Normalized, bacteria (Dill 2011) | $T_{min}$ and $T_{max}$ are not defined $T_{opt}$ is found numerically | Yes (implicit) |
| Heat capacity based | M | 4 | 12, Soil processes (Schipper et al. 2014) | $T_{min}$, $T_{opt}$, $T_{max}$ are found numerically | No |

'Validation' corresponds to the original data sets used to develop and validate the models

*E* empirical models, *M* mechanistic models, *SE* semi-empirical models

**Table 2** Comparison of the main models for growth rate as a function of temperature (see also Sect. 3.1)

| Model | Calibration | $r^2$ | \|AIC\| | \|BIC\| | # Citations |
|---|---|---|---|---|---|
| Empirical models | | | | | |
| Square-root | **** | 0.987 | 50.694 | 49.906 | 710 |
| CTMI | ***** | 0.989 | 52.541 | 51.752 | 267 |
| Blanchard | **** | 0.988 | 50.092 | 49.303 | 111 |
| Bernard and Rémond | ***** | 0.989 | 52.541 | 51.752 | 77 |
| Eppley–Norberg | **** | 0.988 | 52.064 | 51.275 | 146 |
| Semi-empirical models | | | | | |
| Arrhenius equation | – | – | – | – | – |
| General mechanistic models | | | | | |
| Master reaction | *** | 0.944 | 33.443 | 32.457 | 107 |
| Hinshelwood | ** | 0.945 | 37.946 | 37.157 | 507 |
| DEB theory | * | 0.985 | 33.748 | 32.368 | – |
| Protein-stability based models | | | | | |
| Modified Master reaction | *** | 0.841 | 26.403 | 25.417 | 20 |
| Proteome based | ** | 0.839 | 30.064 | 29.472 | 126 |
| Heat capacity based | ** | 0.841 | 26.429 | 25.443 | 42 |

$r^2$, |AIC| (Akaike Information Criterion) and |BIC| (Bayesian Information Criterion) are the absolute values calculated for Fig. 2. 'Calibration' corresponds to calibration easiness, rated from 1 to 5 stars (the latter being better); calibration easiness is determined using several criteria: the associated computing time, the existence of a dedicated algorithm, the identifiability of the model, the biological meanings of the parameters. The number of citations is estimated using Google Scholar citations for the first article presenting the model

### 2.1 Experimental and methodological clarifications

The specific growth rate is defined, in batch acclimated cultures, as the specific biomass growth rate during the exponential phase:

$$\mu(T) = \frac{1}{X}\frac{dX}{dt} = \frac{\ln(2)}{g(T)} \quad (1)$$

where $T$ is a fixed temperature, $X$ is the biomass concentration and $g(T)$ is the generation time (i.e the time it takes to double the population size). The organisms are assumed to be in balanced growth conditions as defined by Campbell (1957) (i.e. every extensive property of the growing system increases by the same factor over a time interval), for a period long enough so that the acclimation processes have reached their steady state. $\mu(T)$ is commonly called the thermal growth curve or the thermal reaction norm (Kingsolver 2009).

It is important to note that in practice the thermal growth curve depends on different factors, especially the way biomass is measured. Firstly, different biomass descriptors are commonly used, such as cell counts, particulate organic carbon concentration (POC), total cell biovolume or optical density. The dynamics of some descriptors is likely to be affected differentially by temperature than, for example, the dynamics of cell concentration. In phytoplankton, the chlorophyll content is a function of temperature (Geider 1987), and thus the evolution of optical density results both from the growth process and from the shift in the cellular optical properties. An ideal biomass estimate should be proportional to the carbon mass with a temperature-independent constant. The difficulty to compare observations from different studies is inherent to heterogeneity in the measured descriptors.

Secondly, the experimental protocols are most of the time unclear on the acclimation period preceding the growth measurement. Acclimation time can vary from one day to several weeks (Boyd et al. 2013; Corkrey 2014). In some cases, biomass evolution is probably affected by acclimation to the new

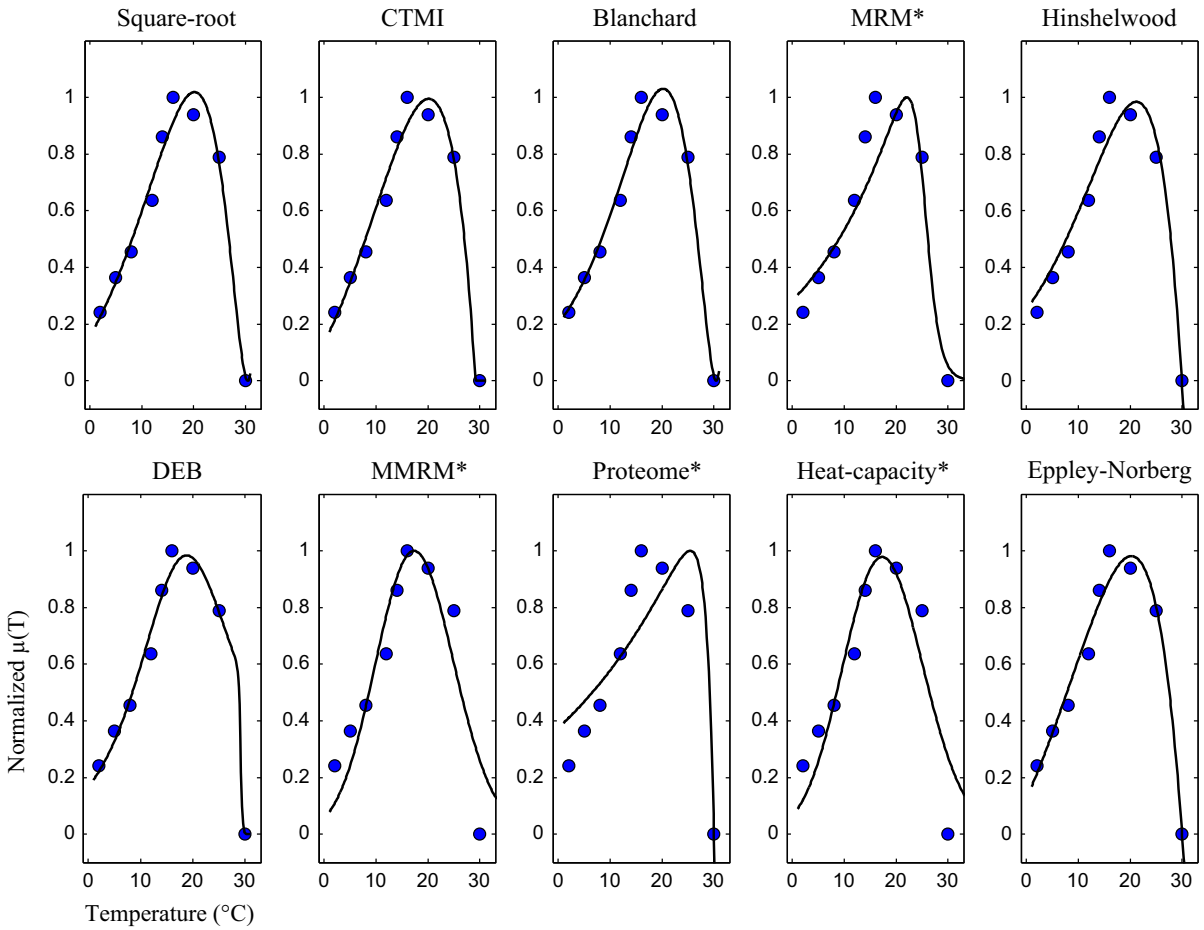


**Fig. 2** Fit of the 10 described models on the normalized thermal growth curve of *Asterionella formosa* [extracted from Bernard and Rémond (2012)]. Models denoted with a * are normalized. *MRM* master reaction model, *MMRM* modified master reaction model

temperature. For example, some experimental protocols proceed by gradually increasing temperature and measuring the growth rate. The main advantage is that they provides a rapid evaluation of the temperature response, but the recorded response reflects a mix between a transient acclimation phase and the effect of temperature on the cell metabolism. The possible bias is however even stronger when the descriptor used is related to carbon content with a temperature-dependent constant. For example, a too short period of acclimation results in a still evolving biomass to chlorophyll a ratio. Therefore, if the growth rate is estimated using chlorophyll a concentration (or turbidity) the computed growth rate will be biased.

The growth rate estimated from oxygen production must also be considered with care. The light phase of photosynthesis is mainly a photochemical process and is hardly affected by temperature at temperatures below $T_{opt}$. Carbon dioxide fixation in the Calvin cycle is an enzymatic process which is highly temperature dependant. Estimating growth rate from oxygen production will thus mask most of the temperature impact if an acclimation period has not been considered. The experimental acclimation period at a given temperature is of major importance for the consistency of the thermal growth curve.

For all these reasons, Boyd et al. (2013) have developed a protocol to construct the thermal growth curve for phytoplankton and optimize the comparability of different thermal growth curves between different experiments and different species. This protocol specifies that:

1. the population must be acclimated to the experimental temperature for at least 4 generations (we recommend even 7 generations),
2. the population must be kept at an exponential growth phase using semi-continuous cultures,
3. multiple biomass descriptors must be used and compared to obtain growth rates (cell counts, chlorophyll a fluorescence, etc.); we recommend to consider carbon or dry weight for biomass,
4. a minimum of 6 experimental growth rates at 6 different temperatures must be obtained,
5. the cultures must be carried out with three replicates,
6. all the other parameters must be kept constant, if possible at optimal levels,
7. the experiments with temperatures at which the cells do not grow or grow very slowly must be repeated several times,
8. several strains of the same species should be compared.

## 2.2 Empirical approach to model the thermal growth curve

Various empirical models (i.e. not developed from biological assumptions) have been proposed since the 1960's to represent the thermal growth curve, but only three are still commonly used. Historically, these models have mostly been developed for food-processing industry and medical applications.

*The square-root model* The Square-Root model was initially proposed by David Ratkowsky as an alternative to the Arrhenius model (Ratkowsky et al. 1982) (see Eq. 9) and then extended to the whole biokinetic range (Ratkowksy et al. 1983):

$$\mu(T) = \left[b\left(T - T_{min}\right)\left(1 - e^{c(T-Tmax)}\right)\right]^2 \quad (2)$$

with

$$T_{min} \leq T \leq T_{max} \quad (3)$$

where $T_{min}$ and $T_{max}$ are the minimal and maximal temperatures for growth, $b$ is the regression coefficient of the squared root growth rate plotted against temperatures below the optimal temperature, and $c$ is an additional parameter to represent growth rate decrease above the optimal temperature.

*The CTMI model* The CTMI (Cardinal Temperature Model with Inflexion) was developed by Lobry et al. (1991) and later popularized by Rosso et al. (1993):

$$\begin{cases} \mu(T) = 0 & \text{if } T < T_{min} \\ \mu(T) = \mu_{opt}\phi(T) & \text{if } T_{min} \leq T \leq T_{max} \\ \mu(T) = 0 & \text{if } T > T_{max} \end{cases} \quad (4)$$

with

$$\phi(T) = \frac{(T - T_{max})(T - T_{min})^2}{(T_{opt} - T_{min})\left[(T_{opt} - T_{min})(T - T_{opt}) - (T_{opt} - T_{max})(T_{opt} + T_{min} - 2T)\right]} \quad (5)$$

under the condition (Bernard and Rémond 2012):

$$T_{opt} > \frac{T_{min} + T_{max}}{2} \quad (6)$$

$T_{min}$, $T_{opt}$, $T_{max}$ are the minimal, optimal and maximal temperature for growth and $\mu_{opt}$ is the growth rate at $T_{opt}$. The model parameters have a direct biological interpretation. The model was built for an easy calibration on experimental data.

*The Blanchard model:* The Blanchard model was developed by Blanchard et al. (1996) to model the photosynthetic capacity of benthic phytoplankton as a function of temperature. This model can be used to represent the thermal growth curve:

$$\mu(T) = \mu_{opt}\left(\frac{T_{max} - T}{T_{max} - T_{opt}}\right)^{\beta} e^{-\beta(T_{opt} - T)/(T_{max} - T_{opt})} \quad (7)$$

with $T \leq T_{max}$ and $T_{opt} < T_{max}$. Parameters $T_{opt}$ and $T_{max}$ correspond to the cardinal temperatures, $\mu_{opt}$ is the growth rate at $T = T_{opt}$ and $\beta$ is a dimensionless parameter.

*The Eppley–Norberg model* Eppley (1972) reviewed the effect of temperature on phytoplankton growth in the sea by comparing different thermal growth curves for a variety of phytoplankton species

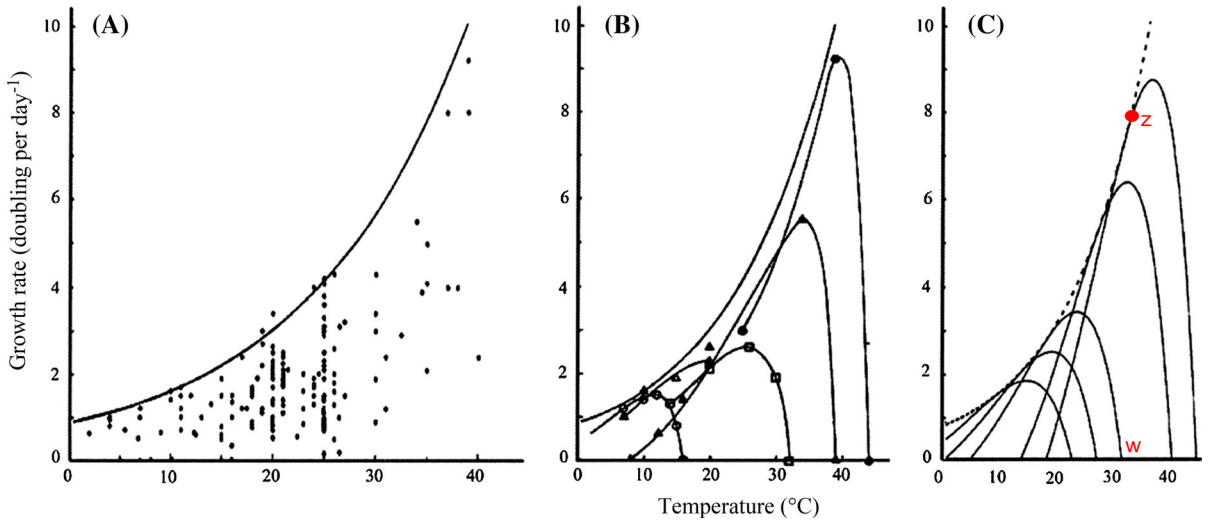


**Fig. 3** **a** Eppley envelope function with the original data points. **b** 5 Data sets for eukaryotic phytoplankton species. **c** Eppley–Norberg plot for the 5 species [redrawn from Norberg (2004)]

in non-limiting conditions (nearly 200 data points). Eppley (1972) determined that the maximal growth rate $\mu_{opt}$ for each species is constrained by a virtual envelope along the optimal temperature trait $T_{opt}$, the so-called 'Eppley curve' (see Fig. 3). Eppley (1972) stated that for any phytoplankton species growing under 40 °C, 'hotter is faster'.

Using Eppley's hypothesis, Norberg (2004) developed a temperature-growth model, the 'Eppley–Norberg' model:

$$\mu(T) = \left[1 - \left(\frac{T - z}{w}\right)^2\right] ae^{bT} \quad (8)$$

where $w$ is the thermal niche width, $z$ is the temperature at which the growth rate is equal to the Eppley function and is a proxy of $T_{opt}$, $a$ and $b$ are parameters of the Eppley function. The Eppley–Norberg model is widely used by the scientific community working on phytoplankton [e.g. see the recent paper of Taucher et al. (2015)].

## 2.3 Empirical model comparison

A comparison between the Square-Root model and the CTMI was made by Rosso et al. (1993) and more recently by Valik et al. (2013). According to these studies, the two models fit equally well the data. Both models are validated by Valik et al. (2013) using an F-test. However, the $b$ and $c$ parameters of the Square-root model are correlated, whereas the CTMI parameters are not, which allows easier parameter identification.

A more extensive comparison between the set of empirical models is presented on Fig. reftimbre2 for *Asterionella formosa*. It turns out that most of them can successfully describe this data set, but the fit is almost perfect for the CTMI and the Square-Root model. The CTMI proves useful for cardinal temperatures identification since all these parameters have a biological meaning. A guideline for choosing the most appropriate model is proposed in the discussion section.

## 2.4 Semi-empirical approach

Semi-empirical models use a combination of biological mechanisms and empirical formulations. The very first temperature model, the Arrhenius equation, was developed in this way.

*The Arrhenius equation* In the beginning of the twentieth century, the work of Jacobius Van't-Hoff and Svante Arrhenius on the effect of temperature on chemical reactions (Arrhenius 1889) was introduced in biology by Snyder (1906), setting that temperature has an exponential influence on biological reactions and then on cellular growth according to the following equation called 'the Arrhenius law':

$$k(T) = Ae^{-E/(RT)} \quad (9)$$

where $k(T)$ is the rate of reaction, $R$ is the gas constant, $A$ is called the 'collision factor' or the pre-exponential part and $E$ is the activation energy, determined empirically. The Arrhenius equation is semi-empirical, partially based on thermodynamical considerations; it can be interpreted as the number of collisions per unit of time multiplied by the probability that a collision results in a reaction. The Arrhenius equation is widely used to describe the temperature effect on different biological processes, from enzyme catalysis to community activity (e.g. see Frauenfelder et al. 1991; Lloyd and Taylor 1994; Gillooly et al. 2001). However, it is only valid on a small range of temperature, excluding high temperatures inhibiting growth (Slator 1916). Arrhenius model parameters are easy to estimate using an Arrhenius plot, by expressing $\ln(\mu(T))$ as a function of $1 / T$, which gives a linear relationship; parameters can thus be obtained with a linear regression. The Arrhenius model allows good representations of growth rates at low temperatures, but some Arrhenius plot does not give straight lines, indicating for example that $E$ can vary with $T$. Moreover, the Arrhenius model cannot represent the decreasing part of the thermal growth curve, e.g. when temperature causes cell death. Arrhenius equation can be conveniently reformulated as:

$$k(T) = k_r e^{T_A/T_r - T_A/T} \quad (10)$$

where $T_r$ is a reference temperature, $T_A$ is the Arrhenius temperature (i.e. slope of the straight line of the Arrhenius plot) and $k_r$ is the reaction rate at $T_r$.

## 2.5 Mechanistic approach

The empirical models are convenient to identify the main characteristics of the thermal growth curve. However, the mechanistic approach aims to represent the thermal growth curve as a result of the inherent physiological processes. These models are mostly based on the Arrhenius formulation, but also on the Eyring equation. In addition to their explanatory role, because their parameters have thermodynamical meanings, it is possible to extract thermodynamical informations from the thermal growth curve only.

### 2.5.1 *General models based on the Arrhenius and Eyring formulations*

*The Eyring equation and the Transition-State theory* this theory stipulates that, during a chemical reaction, there exists an intermediate form between the reactants and the products (e.g. the native and denatured protein and enzyme) which is in rapid equilibrium with the reactants (Eyring 1935):

$$P_f \underset{k_2}{\overset{k_1}{\rightleftharpoons}} TS \xrightarrow{k_d} P_u \quad (11)$$

where, in this example, $P_f$ and $P_u$ are the fraction of native and denatured proteins, respectively, and $TS$ is the transition state. The Eyring equation, roughly similar to the Arrhenius law, was nonetheless based on these pure mechanistic considerations and reads (Eyring 1935):

$$k(T) = \frac{K_B T}{h} e^{\Delta S^{\ddagger}/R} e^{-\Delta H^{\ddagger}/(RT)} \quad (12)$$

where $K_B$ is the Boltzmann constant, $h$ is the Planck's constant. The parameters $\Delta S^{\ddagger}$ and $\Delta H^{\ddagger}$ correspond to the entropy and enthalpy of activation for the transition state.

*The master reaction model* Johnson and Lewin (1946) noticed that cultures of *Escherichia coli* exposed to 45 °C during a long time ceased to grow, but grew exponentially again when replaced at 37 °C. The longer the cultures were exposed to the high temperature, the lower was the growth rate at 37 °C. However, there was no sign of viability loss. They concluded that cells endured reversible damage, particularly protein denaturation. They considered a simple case where a single reaction controlled by one master enzyme $E_n$ limits growth (with no substrate limitation):

$$\mu(T) = cTE_n e^{-\Delta H_A^{\ddagger}/(RT)} e^{\Delta S_A^{\ddagger}/R} \quad (13)$$

where $c$ is a constant given by the Eyring formulation (Eyring 1935), $\Delta H_A^{\ddagger}$ is the enthalpy of activation (enthalpy difference between the transition complex and the active form) and $\Delta S_A^{\ddagger}$ is the entropy of activation.

The enzyme goes from a native, active form $E_n$ to a reversibly denatured, inactive form $E_d$:

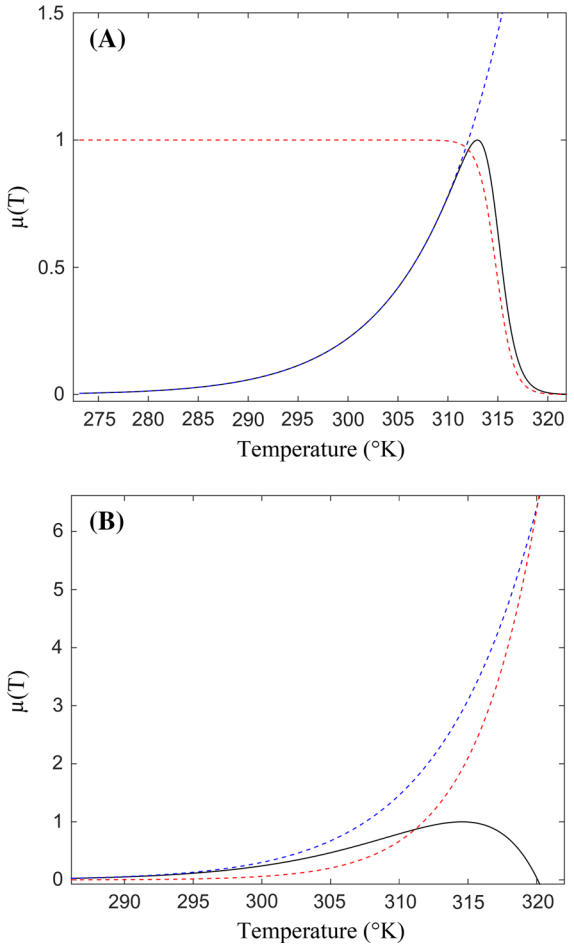


**Fig. 4** Illustration of the master reaction model (**a**) and of the Hinshelwood model (**b**). The black lines correspond to $\mu(T)$, the blue dashed lines corresponds to $CTe^{-\Delta H^{\ddagger}/(RT)}$ (**a**) and to $f_1(T)$ (**b**), the red dashed line corresponds to $P(T)$ (**a**) and to $f_2(T)$ (**b**). (Color figure online)

$$E_n \underset{k_2}{\overset{k_1}{\rightleftharpoons}} E_d \tag{14}$$

The chemical equilibrium is defined as:

$$K = k_1/k_2 = E_d/E_n = e^{-\Delta H/(RT)+\Delta S/R} \tag{15}$$

where $\Delta H$ is the enthalpy difference between the active form and the inactive form, $\Delta S$ is the entropy difference. If $E_0$ is the total amount of enzyme, $E_0 = E_n + E_d$. It follows that:

$$E_n = \frac{E_0}{1+K} = \frac{E_0}{1+e^{-\Delta H/(RT)+\Delta S/R}} \tag{16}$$

Then, by posing $C = ce^{\Delta S_A^{\ddagger}/R}E_0$ and replacing $E_n$ by Eq. 16 in 13, Johnson and Lewin obtained the master reaction model (see Fig. 4a):

$$\mu(T) = CTe^{-\Delta H_A^{\ddagger}/(RT)} \cdot \underbrace{\frac{1}{1+e^{-\Delta G(T)/(RT)}}}_{P(T)} \tag{17}$$

where $P(T)$ is the probability that the enzyme is in its native state and $\Delta G(T)$ is the Gibbs free energy change:

$$\Delta G(T) = \Delta H - T\Delta S \tag{18}$$

However, the master reaction model assumes that $\Delta G$ is temperature independent. An other version of Eq. 17 exists, where the exponential part does not follow an Eyring formulation but rather an Arrhenius one, which is relevant in the case of reactions with high activation energy like protein denaturation (Bischof and He 2005):

$$\mu(T) = Ce^{-\Delta H_A^{\ddagger}/(RT)} \cdot \frac{1}{1+e^{-\Delta G(T)/(RT)}} \tag{19}$$

It is worth noting that this equation here simplifies the calculation of the cardinal temperature $T_{opt}$ and is supposed to have little influence on the model fit and behavior (see Tables 1, 2).

*The Hinshelwood model* Hinshelwood (1945) proposed a rather simple model in which the temperature-dependent growth rate is just the difference between a synthesis rate $f_1(T)$ and a degenerative rate $f_2(T)$ (see Fig. 4b):

$$\mu(T) = \overbrace{A_1 e^{-E_1/(RT)}}^{f_1(T)} - \underbrace{A_2 e^{-E_2/(RT)}}_{f_2(T)} \tag{20}$$

where $A_1$ and $A_2$ are related to entropy and $E_1$ and $E_2$ are related to enthalpy. Hinshelwood believed that the function $f_2(T)$, which causes the '*catastrophic decline to zero*' (Hinshelwood 1945), represents protein denaturation. He argued that the model only works if $E_2$ is higher than $E_1$, because the degenerative process represented by $f_2(T)$ must be sudden. Since protein denaturation possesses a high activation energy, it is a good candidate for driving the process. Moreover, $A_2$ (corresponding to entropy) also has to be quite high. Thus, the '*activated state must be highly disordered compared with the initial state*' which '*results in an easy transition to the activated state in spite of the*

*large amount of energy which has to be taken up to reach it*' (Hinshelwood 1945). Precisely, protein denaturation leads from a highly ordered state to an higly disordered state and is therefore associated with a large entropy increase. From the Hinshelwood model, after some mathematical manipulations, it is possible to express $T_{min}$, $T_{opt}$, $T_{max}$ (see Table 1).

*The DEB theory approach* In the Dynamics Budget Theory, the effect of temperature on population growth is taken into account using a modified Master Reaction model (Kooijman 2010), where all the temperature-dependent functions are Arrhenius modified equations:

$$\mu(T) = \frac{k_1 e^{T_A/T_1 - T_A/T}}{\underbrace{1 + e^{T_{AL}/T - T_{AL}/T_L} + e^{T_{AH}/T_H - T_{AH}/T}}_{f_D}} \quad (21)$$

where $T_L$ and $T_H$ are related to cold and hot denaturation (lower and upper boundaries), $T_{AL}$ and $T_{AH}$ are the Arrhenius temperatures (i.e. the slope of the straight line of the Arrhenius plot at low and high temperatures respectively, see eq. 10). The ratio $f_D^{-1}$ corresponds to the fraction of enzyme in its native state. This model therefore also accounts for cold denaturation, contrary to the Master Reaction model.

### 2.5.2 *The protein thermal stability hypothesis*

In addition to the temperature-dependent enzyme activity, protein thermal stability plays a key role in the microbial thermal growth curve (Johnson and Lewin 1946; Rosenberg et al. 1971; Zeldovich et al. 2007; Pena et al. 2010). If temperature increases, certain proteins become first inactive and then denatured. Especially, at high temperatures ($T > T_{opt}$), this phenomenon occurs for many proteins and causes a growth rate decrease. In line with the master reaction model, some models include additional assumptions about protein thermal stability and its consequences on growth, assuming that proteins are the key factors controlling thermal growth curves.

*The modified master reaction model* The master reaction model assumes that $\Delta G$, the Gibbs free energy difference between the native and denatured protein, is temperature independent. Based on Murphy et al. (1990) work, Ross (1993) and then Ratkowsky et al. (2005) remarked that $\Delta G$ should vary with $T$ in Eq. 17 following 18. Moreover, Murphy et al. (1990) showed that globular proteins (including enzymes) share common thermodynamic properties. For any protein, the denaturation enthalpy change ($\Delta H$) and the denaturation entropy change ($\Delta S$), normalized to the number of amino-acids residues of this protein, both converge to a fixed value $\Delta H^*$ and $\Delta S^*$ at $T_H^*$ and $T_S^*$ respectively (Privalov 1979). The reason for such a temperature convergence is still unclear. Nonetheless, it has been shown that, at $T_H^*$ and $T_S^*$, the hydrophobic contribution to $\Delta H$ and $\imath S$ approaches zero (Robertson and Murphy 1997). Using the heat capacity thermodynamic parameter $C_p$, Murphy et al. (1990) stated that $\Delta H$ and $\Delta S$ can be expressed as a function of the heat capacity change $\Delta C_p$:

$$\Delta H = \Delta H^* + \Delta C_p (T - T_H^*) \quad (22)$$

$$\Delta S = \Delta S^* + \Delta C_p \ln(T/T_S^*) \quad (23)$$

where $\Delta H^*$ is the enthalpy change per mol of amino-acid residue of the enzyme at $T_H^*$, $\Delta S^*$ is the entropy change per mol of amino-acid residue of the enzyme at $T_S^*$, $\Delta C_p$ is the heat capacity difference between the native and denatured protein, $T_H^*$ is the temperature at which the contribution of $\Delta C_p$ to enthalpy is zero and $T_S^*$ is the temperature at which the contribution of $\Delta C_p$ to entropy is zero. The heat capacity change $\Delta C_p$ is constant for a given protein (Privalov and Khechinashvili 1974). Using Eqs. 22 and 23, the Gibbs free energy of protein denaturation (i.e. the protein thermal stability) is (Fig. 5):

$$\Delta G(T) = n\left[\Delta H^* - T\Delta S^* + \overbrace{\Delta C_p[(T - T_H^*) - T\ln(T/T_S^*)]}^{\Delta G_{hydro}}\right] \quad (24)$$

where $n$ is the number of amino-acid residues in the master enzyme and $\Delta G_{hydro}$ is the hydrophobic contribution to the free energy change. Equation 24 describes protein thermal stability in terms of hydrophobic contribution of apolar compounds.

Ross (1993) and Ratkowsky et al. (2005) proposed to replace $\Delta G$ by Eq. 24 in 17 (forming the modified master reaction model). Because $T_H^*$, $T_S^*$ and $\Delta S^*$ are considered as universal constant for globular proteins (Murphy and Gill 1991), the modified master reaction model has 5 tunable parameters (Fig. 5). As a validation, Ratkowsky et al. (2005) fitted the model on 35 bacterial strains normalized data sets obtained in

non-limiting conditions. Their main conclusion points towards the crucial role played by a single master enzyme whose thermal sensitivity is driven by hydrophobic interactions.

Corkrey (2014) extended the modified master reaction model to unicellular and multicellular eukaryotes. They considered $\Delta H^*$ as a universal constant as well, reducing the model parameters to 4. They fitted the model on 230 strains normalized data sets covering a range of 124 °C. Their principal conclusion states that the model is able to find coherent protein thermodynamics parameters with only net growth rates data (i.e. growth rate versus temperature). Hyperthermophiles proteins seem to be more widely robust. Moreover, they found several links between thermodynamic parameters, for example between $T_{opt}$ and $\Delta C_p$ (enzyme stability), and between $T_{opt}$ and $\Delta H^{\ddagger}$ (enzyme activity). However, they did not provide further explanations. They finally speculate on the nature of the single limiting reaction. They assume that if a single reaction (and not several) is rate limiting, then it should be linked to the protein unfolding and re-folding process. They particularly focus on the role of chaperones proteins responsible for de novo folding.

*The proteome-scale approach* Zeldovich et al. (2007) proposed that the whole proteome plays a role in microbial thermal sensitivity. Resuming this idea, Chen and Shakhnovich (2010) considered that each

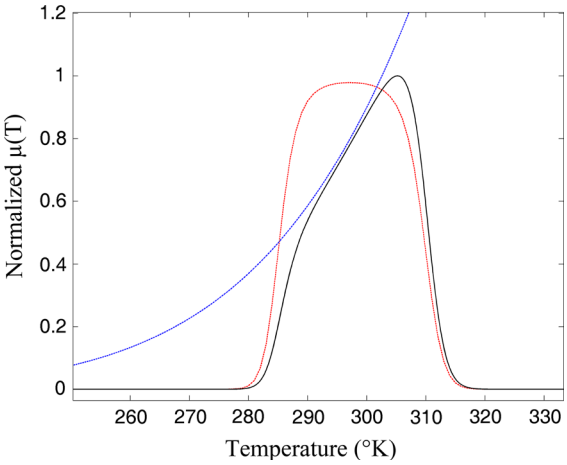


**Fig. 5** The modified master reaction model plot for a microbial species (black line) with activation function (blue dashed line) and protein denaturation probability $P(T)$ (red dashed line). (Color figure online)

important protein $i$ has its own Gibbs free energy of denaturation $\Delta G_i$. The growth rate of a microbe becomes dependent of the stability of each protein, and the thermal denaturation of several proteins causes a bottleneck effect on growth:

$$\mu(T) = CTe^{-\Delta H^{\ddagger}/(RT)} \cdot \frac{1}{\prod_i^{N_p} 1 + e^{-\Delta G_i(T)/(RT)}} \tag{25}$$

where $N_p$ is the number of proteins. According to Zeldovich et al. (2007), the proteome can be described in protein stability distribution thanks to a dedicated probability function of the Gibbs free energy, $P(\Delta G)$ (see Fig. refprotherm). By taking the natural logarithm of Eq. 25, Chen and Shakhnovich (2010) expressed the growth rate as:

$$\ln(\mu(T)) = \ln(CT) - \Delta H^{\ddagger}/(RT) - \sum_{i=1}^{N_p} \ln\left(1 + e^{-\Delta G_i/(RT)}\right) \tag{26}$$

that is, by integrating the resulting equation over the whole $P(\Delta G)$ distribution range and by averaging over the proteome:

$$\ln(\mu(T)) \simeq \ln(CT) - \Delta H^{\ddagger}/(RT) - N_p \int_0^L \ln\left(1 + e^{-\Delta G/(RT)}\right) P(\Delta G)\, \mathrm{d}\Delta \mathrm{G} \tag{27}$$

where $L$ is the maximum value of $\Delta G$ (for example $L = 40$ in Fig. 6). $N_p$ can be reduced to the number of the only important proteins. According to Sawle and Ghosh (2011) and Ghosh and Dill (2010), $\Delta G$ can be expressed as a function of $\Delta H$, $\Delta S$ and $\Delta C_p$ (using Eqs. 22, 23), itself depending on the protein chain length denoted $N$:

$$\Delta G = \Delta H(N) + \Delta C_p(N)(T - T_h) - T\Delta S(N) - T\Delta C_p(N)\ln(T/T_s) \tag{28}$$

with

$$\begin{aligned} \Delta H(N) &= aN + b \\ \Delta S(N) &= cN + d \\ \Delta C_p(N) &= lN + m \end{aligned} \tag{29}$$

where $a$, $b$, $c$, $d$, $l$, $m$ are empirical parameters defined for mesophilic and for thermophilic organisms. The distribution of chain length over the

proteome $P(N)$ can be known (Zhang 2000) and is used to estimate $P(\Delta G)$. It can be modelled by a gamma distribution:

$$P(N) = \frac{N^{\alpha-1}e^{-N/\theta}}{\Gamma(\alpha)\theta^{\alpha}} \tag{30}$$

where $\theta$ and $\alpha$ are the parameters of the gamma distribution corresponding to:

$$\begin{aligned} \langle N \rangle &= \alpha\theta \\ \langle (\Delta N)^2 \rangle &= \alpha\theta^2 \end{aligned} \tag{31}$$

The brackets represent the mean over all the proteins. $\Gamma(\alpha)$ is the gamma function evaluated at $\alpha$. The model (Eq. 27), presented as universal, has thus only two parameters, $N_p$ and $\Delta H^{\ddagger}$. It has been validated on 12 normalized data sets of prokaryotes.

*The heat capacity hypothesis* Hobbs et al. (2013) and Schipper et al. (2014) proposed a model called the Macromolecular Rate Theory (MMRT) in which the thermal growth curve is driven by the heat capacity change of activation $\Delta C_p^{\ddagger}$ (i.e. the heat capacity difference between the ground state and the transition state). More precisely, the growth rate is expressed as:

$$\mu(T) = \frac{k_B}{h} T e^{\Delta G^{\ddagger}(T)/(RT)} \tag{32}$$

where $k_B$ and $h$ are the Boltzmann and Planck's constants, $\Delta G^{\ddagger}$ is the Gibbs free energy difference between the ground state and the transition state of a possible rate-limiting enzyme. Contrary to the master reaction model, the MMRT considers that enzymes do not denature easily and are in rapid equilibrium with a folded, inactive intermediate (i.e. the transition state). The Gibbs free energy difference can be here written as:

$$\Delta G^{\ddagger}(T) = \Delta H^{\ddagger}_{T_0} + \Delta C_p^{\ddagger}(T - T_0) + T(\Delta S^{\ddagger}_{T_0} + \Delta C_p^{\ddagger} \ln(T/T_0)) \tag{33}$$

If $\Delta C_p^{\ddagger} > 0$, then the heat capacity difference between the ground state and the transition state (i.e. the inactive folded enzyme) itself is sufficient to explain the decrease of growth rate above $T_{opt}$. Schipper et al. (2014) validated the MMRT model on microbial soil processes data sets.

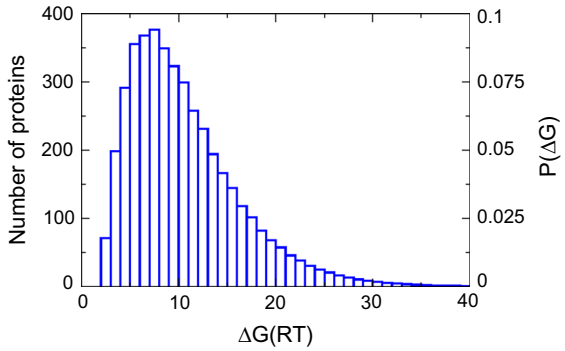


**Fig. 6** Gibbs free energy distribution of *Escherichia coli* proteome at 37 °C [adapted from Ghosh and Dill (2010)]

## 2.6 Mortality induced by temperature

Warm temperatures increase cell mortality because of protein denaturation and membranes injuries. For phytoplankton, photosystems and electron chain transport are denaturated (Song et al. 2014), and a transient imbalance between the energy needed and produced must be managed by the cell (Ras et al. 2013; Smelt and Brul 2014; Serra-Maia et al. 2016).

So far, models explicitly presenting the mortality rate as a function of temperature are rare. The Hinshelwood model explicitly integrates a mortality rate with an Arrhenius law (see Fig. 7b). This model turned out to efficiently represent mortality together with growth for the chlorophyta *Chlorella vulgaris* (Serra-Maia et al. 2016). Another example is Uden (1985) who combined a master reaction growth model and an exponential death model for yeast:

$$\mu(T) = \frac{Ce^{-\Delta H^{\ddagger}/(RT)}}{1 + e^{-\Delta G/(RT)}} - \frac{k_B T}{h} e^{\Delta S^{\ddagger}_{den}/R - \Delta H^{\ddagger}_{den}/(RT)} \tag{34}$$

where $\Delta S^{\ddagger}_{den}$ and $\Delta H^{\ddagger}_{den}$ are the entropy and enthalpy of activation of cells mortality.

Outside of the thermal niche width, for temperatures above the species $T_{max}$, the kinetics of cell inactivation is called the survival curve (Moats 1971) (Fig. 7a); from each survival curve, it is possible to infer the mortality rate at a given temperature. Different empirical models have been developed, especially in food science, to represent these survival curves (Mafart et al. 2002; Smelt et al. 2002; Smelt and Brul 2014).

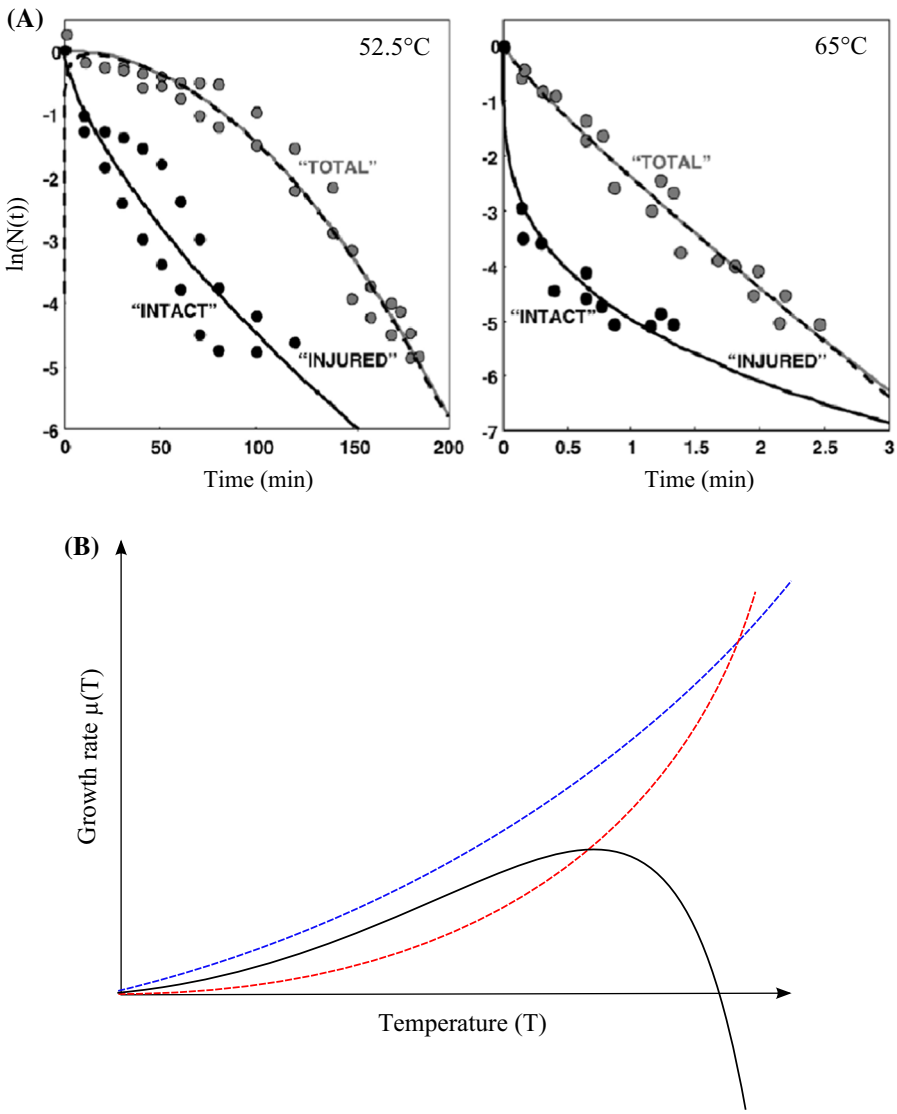


**Fig. 7** **a** Survival curves at different temperatures for *Listeria innocus* (redrawn from Corradini and Peleg (2006)). **b** Hinshelwood model (black curve) with mortality (red curve) as in Serra-Maia et al. (2016). (Color figure online)

## 3 Choosing the most appropriate model

In this section, we propose a guideline for choosing the most appropriate model depending on the study objectives. We summarize and compare the models performance and their applicability to phytoplankton under different modeling scenarios, and highlight the most appropriate models.

The model comparison is based on the analysis of 193 thermal curve responses associated to 193 different strains, resulting from 130 species (Thomas et al. 2012). This data set includes the main phyla of unicellular photosynthetic organisms.

An illustration of the model performance for 5 strains of the cyanobacterium genus *Synechococcus* sp. is plotted on fig. S1 (Pittera et al. 2014).

### 3.1 Synthesis of model performance

Three criteria have been considered to assess a model efficiency. The absolute model performance is estimated using $r^2$. To account both for the fit quality and the number of parameters, we considered the Akaike Information Criterion (AIC) (Akaike 1992) and the Bayesian Information Criterion (BIC) (Schwarz 1978) (see Table 3; table S1-S3). The best models are,

globally, the empirical models, and the Eppley–Norberg and the CTMI turn out to obtain the best score (see table S2, fig. S2). The Hinshelwood model, in the other way, has the best score among the mechanistic models. It is worth noting here that the CTMI assumes that $T_{max} - T_{opt} \leq T_{opt} - T_{min}$, which is not the case for the Eppley–Norberg. Thus, for small data sets with few points near $T_{opt}$, the Eppley–Norberg model has a better fit score (see fig. S3).

To highlight the combination of fit quality and other important characteristics, we defined several criteria in Tables 1 and 2: number of parameters, validation on experimental data, mathematical expression of the cardinal temperatures, assumption regarding mortality, calibration easiness, fit quality using $r^2$, AIC, BIC, and number of citations. From these criterions, we could derive advantages, limitations and rating for each model (Table 3). The CTMI, Bernard&Rémond and the Hinshelwood model obtain the highest score, with the best trade-off between complexity (e.g. few parameters), fit quality, calibration easiness and parameters interpretation.

### 3.2 Macroscopic modeling without including mortality

A common scenario when modeling the effect of temperature on phytoplankton is the need of representing the net thermal response, without explicitly representing mortality. The response is generally focusing on growth rate, but it can also represent a detailed physiological processes. Below the optimal temperature, the Arrhenius equation has been widely used, has a good fit, is easy to calibrate and its parameters can be interpreted. However, to represent the whole thermal growth curve, the CTMI is the best choice because its parameters are directly the cardinal temperatures and its calibration is easily possible thanks to a dedicated algorithm. The Eppley–Norberg model is also a relevant choice with very similar goodness of fit, especially to describe growth in optimal light conditions. However, the calibration of this model is less straightforward than the CTMI. When light is not photoinhibiting, these models can be easily combined with the light effect on growth. In particular, the Bernard and Rémond model is a good trade-off. This latter model has been originally validated on 15 phytoplankton species and here on 193 phytoplankton species (table S1-S3) from the main phytoplankton phyla. The CTMI is thus expected

**Table 3** Advantages, limitations and rating of the main models for growth rate as a function of temperature

| Model | Advantages | Limitations | Rating |
|---|---|---|---|
| Square-root | Fit quality | No mortality, $T_{opt}$ is not easily defined | *** |
| CTMI | Fit quality, parameters interpretation | No mortality | **** |
| Blanchard | Calibration easiness, fit quality, application to phytoplankton | No mortality $T_{min}$ is not defined | *** |
| Bernard and Rémond | Calibration easiness, fit quality, parameters interpretation, application to phytoplankton | No mortality | ***** |
| Eppley–Norberg | Fit quality, application to phytoplankton | No mortality, implicit link between $T_{opt}$ and $\mu_{opt}$ | |
| Arrhenius equation | Fit quality below $T_{opt}$ | No representation of the decreasing phase above $T_{opt}$ | ** |
| Master reaction | Parameters interpretation | $T_{min}$ and $T_{max}$ are undefined | ** |
| Hinshelwood | Fit quality, parameters interpretation, explicit mortality | $T_{min}$ is not defined | **** |
| DEB theory | Fit quality | High number of parameters | * |
| Modified Master reaction | Parameters intepretation | Poorness of fit | ** |
| Proteome based | Parameters intepretation, only 2 parameters | Poorness of fit | *** |
| Heat capacity based | – | Poorness of fit, parameters interpretation not clear | * |

Rating is based on criteria from Tables 1 and 2 (fit quality and calibration easiness), from 1 to 5 stars (the latter being better)

to be the ideal candidate to represent the effect of temperature on phytoplankton communities. The Eppley–Norberg model is also interesting for modeling communities as two of its four parameters are considered universal and only two are strain-specific.

### 3.3 Macroscopic modeling with explicit mortality rate

As we pointed out, few studies exist to represent the effect of temperature on phytoplankton mortality. The only model that explicitly represents mortality is the Hinshelwood model. Adapted for phytoplankton (Serra-Maia et al. 2016), this model is thus recommended because its parameters can be interpreted, and the fit quality is acceptable; however, its parameters calibration are not easy on experimental data with few data points. We thus recommend to use the CTMI to generate a patron for the net growth rate. The patron, made of the data points simulated by the CTMI model can then be advantageously used to calibrate the Hinshelwood model.

### 3.4 Physiological or metabolic modeling

The proteome model is certainly the best candidate to explain the thermal growth curve, as it includes the effect of temperature on the whole proteome and has only two parameters. However, it does not fit very well the experimental data for phytoplankton growth rates compared to the empirical models. As for the Hinshelwood model, a patron can be used to artificially increase the number of data points. This model could also be adapted to phytoplankton when light is photoinhibiting.

## 4 Coupling temperature and other environmental factors

### 4.1 Factors influencing the thermal growth curve

The thermal growth curve is assumed to be obtained in non-limited conditions (Kingsolver 2009). However, some limitations and perturbations usually occur in the environment that may simultaneously involve changes in metabolism. The simplest representation of some multi-factors impact on the growth rate is to assume that all the factors are uncoupled. A classical formalism to represent the effect of $n$ uncoupled factors is given by the gamma concept (Zwietering et al. 1993; Augustin and Carlier 2000):

$$\mu = \mu_{opt} \cdot \prod_{k=1}^{n} \gamma_k \tag{35}$$

where $\mu_{opt}$ is the maximal growth rate when all the $n$ environmental factors are optimal, $\gamma_k$ is a normalized function of the environmental factor $k$. One of the $\gamma_k$ represents the impact of temperature.

In a more accurate approach, the impact of a factor on the cardinal temperatures can be represented (or more generally the parameters of the thermal model can be a function of another factor). In this case, these environmental factors are coupled to temperature. For example, temperature plays a role on oxygen dissolution in water, and the two factors have then a coupled effect on microbial growth rates; this coupling is enhanced for unicellular diazotrophic cyanobacteria which are particularly sensitive to the oxygen concentration, because oxygen inhibits their diazotrophic activity (Brauer et al. 2013).

For the majority of phytoplankton species, the most important physico-chemicals factors are light and nutrients (mainly N and P) (Falkowski and Raven 2013).

### 4.2 The interplay between light and temperature in phytoplankton

Phytoplankton perform oxygenic photosynthesis to harvest light. Photosynthesis metabolism is composed of a dark phase and a light phase, with different thermal sensitivities. The dark phase involves the Rubisco enzyme responsible for $CO_2$ fixation in the Calvin cycle. In the light phase, at low temperatures, the reactions are mainly photochemical and not enzymatic and thus less sensitive to temperature. As a consequence, the cell has to balance the energy and electrons transferred from photons harvesting and their conversion into chemical energy in the dark phase, depending on the temperature [see for example the review by Ras et al. (2013)]. A shift down to low temperatures induces a strong imbalance and thus generates light saturating conditions (see Young et al. 2015). However, at high temperatures, the light phase is strongly affected by temperatures as electron transport chains and photosystems structural stability

is affected (Song et al. 2014) and can induce cell mortality.

#### 4.2.1 *Models assuming an uncoupling between light and temperature effects*

These models assume that temperature and light are independent factors. For example, the model developed by Bernard and Rémond (2012) supposes that the growth rate is expressed as:

$$\mu(T,I) = f(I).\phi(T) \tag{36}$$

where $\phi(T)$ corresponds to the CTMI (Eq. 5) and:

$$f(I) = \mu_{max}\frac{I}{I + \frac{\mu_{max}}{\alpha}\left(\frac{I}{I_{opt}} - 1\right)^2} \tag{37}$$

$\mu_{max}$ is the maximum growth rate at optimal light intensity $I_{opt}$ and optimal temperature $T_{opt}$, $\alpha$ is the initial slope of the light response curve. $f(I)$ was built in line with the Peeters and Eilers (1978) model with photoinhibition, but reparametrized for a better parameter identification. Bernard and Rémond (2012) developed an algorithm to identify the cardinal temperature from data sets with different light conditions. This model was validated on 15 phytoplankton species. The hypothesis of uncoupling is, however, no longer available at high light intensities (i.e. when photoinhibition occurs) as temperature is known to play a role in photoinhibition (Jensen and Knutsen 1993; Edwards 2016).

The model of Eppley–Norberg modified by Follows et al. (2007), uses another formalism to represent both temperature and light effect:

$$\mu(T,I) = \mu_{max}.\underbrace{\frac{1}{\tau_1}\left(A^T e^{-B(T-T_0)^c} - \tau_2\right)}_{\gamma^T}.\underbrace{\frac{1}{\gamma^I_{max}}\left(1 - e^{-k_p I}\right)e^{-k_i I}}_{\gamma^I} \tag{38}$$

where $\mu_{max}$ is the species maximum growth rate, $\gamma^T$ and $\gamma^I$ are respectively the normalized temperature function and the normalized photosynthesis function. The parameters $\tau_1$ and $\tau_2$ ensure the normalization of $\gamma^T$, while parameters $A$, $B$, $T_0$ and $c$ modify its shape by taking into account the Eppley hypothesis (see Fig. 8). Similarly, $\gamma^I_{max}$ ensures the normalization of $\gamma^I$, $1 - e^{-k_p I}$ represents the increase of growth with light at low irradiance and $k_i$ is a constant associated to photoinhibition.

#### 4.2.2 *Models considering a coupling between light and temperature*

The model developed by Dermoun et al. (1992) for the unicellular Rhodophyta *Porphyridium cruentum* accounts for a complex coupling between light and temperature:

$$\mu(T,I) = 2\mu_m(T)(1+\beta_1)\frac{I/I_{opt}(T)}{1 + 2\beta_1 I/I_{opt}(T) + \left(I/I_{opt}(T)\right)^2} \tag{39}$$

where $\mu_m(T)$ is the maximum specific growth rate at a given temperature $T$, $I_{opt}$ is the optimal irradiance at a given temperature $T$ and $\beta_1$ is the shape factor for limiting irradiance. $\mu_m(T)$ and $I_{opt}(T)$ are rational functions (see Dermoun et al. 1992). It is worth noting that the tight coupling between light and temperature in this model leads to identifiability problems partially due to large number of parameters (9 parameters in the model). Furthermore, when light is limiting, the coupling between light and temperature becomes loose.

### 4.3 The interplay between nutrients and temperature

Phytoplankton growth in the oceans is often limited by nitrogen (N) or phosphorus (P). When limiting, these nutrients strongly impact the thermal growth curve (Pomeroy and Wiebe 2001; Thomas 2013; Thomas and Litchman 2016). Trace nutrients such as trace

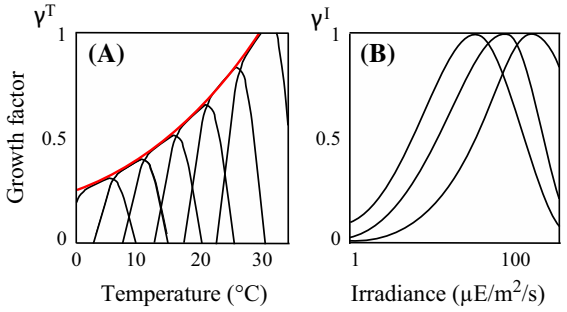


**Fig. 8** **a** Eppley curve normalized at 30 °C. **b** Photosynthesis as represented in Eq. 38. The figure is redrawn after Follows et al. (2007)

metals or essential vitamins can also play an important role on growth but their interplay with temperature is largely unknown.

Thomas (2013) has developed a model taking into account the nutrient effect (N), assuming that anabolism is temperature-dependent and nutrient-dependent, whereas catabolism or mortality only depend on temperature:

$$\mu(T,N) = b_1 e^{b_2 T} \frac{N}{N+K} - (d_1 e^{d_2 T} + d_0) \quad (40)$$

where $b_1$, $b_2$, $d_1$, $d_2$ are Arrhenius parameters for anabolism and catabolism, respectively, and $K$ is the half-saturation constant of a Michaelis–Menten kinetics of nutrient uptake. $d_0$ is a constant catabolism rate independent of temperature. Nutrient limitation leads to a decrease of the thermal niche width, $T_{opt}$ and $\mu_{opt}$ (see Fig. 9a). The model has been validated on temperature and nutrient experiments conducted with the phytoplankton diatom species *Thalassiosira pseudonana* (Thomas et al. 2017).

Grimaud (2016) has developed a dynamical model taking into account temperature and nutrient for eukaryotes phytoplankton species, based on the Droop model (1968). In balanced-growth conditions, the model gives the following thermal growth curve:

$$\mu(T,N) = \frac{\phi_2(T)\phi_1(T)\rho(N)}{\phi_1(T)\rho(N) + \phi_2(T)Q_0} - m \quad (41)$$

where $\phi_1(T)$ and $\phi_2(T)$ are CTMI equations for nutrients and carbon uptake, $\rho(N)$ is a normalized Michaelis–Menten equation, $Q_0$ corresponds to the minimal internal nutrient quota needed to grow, $m$ is the constant mortality/catabolism rate. Figure 9b shows that a nutrient limitation leads to a decrease of $T_{opt}$ and $\mu_{opt}$, in line with Thomas (2013). However, the amplitude of the thermal niche width is less marked, and is only reduced for strong nutrient limitation (see Fig. 9b). Also, these results depend on the difference between $\phi_1(T)$ and $\phi_2(T)$.

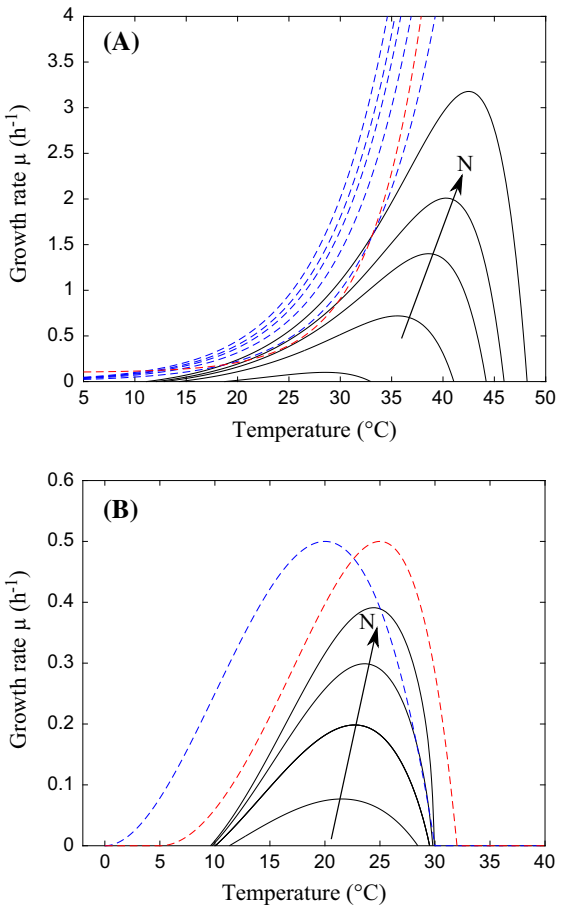


**Fig. 9** Growth rate as a function of nutrient and temperature $\mu(T,N)$. The black lines correspond to different nutrient values, increasing with the arrow. **a** Model of Thomas (2013). The blue and red dashed lines correspond to the positive and negative terms of Eq. 40, respectively. **b** Model of Grimaud (2016). Blue and red dashed lines correspond to $\phi_1(T)$ and $\phi_2(T)$ of Eq. 41, respectively

## 5 Accounting for temperature variations

In the natural environment, cells experience temperature fluctuations at different time-scales, ranging from days to seasons, influencing their physiology and forcing them to acclimate (Ras et al. 2013; Gestel et al. 2013). The question is then how to deal with these variations, while thermal growth curves are obtained in balanced conditions.

### 5.1 Assuming instantaneous acclimation at large time scale

The specific growth rate $\mu(T)$ described in Sect. 2.1 for balanced growth has been used as such when temperature is time-varying, assuming that the effect of temperature is instantaneous [see for example Baranyi and Roberts (1995); Baranyi et al. (1995)]. This approximation is valid in particular for slow variations

of temperature, such as annual fluctuation of sea temperature.

### 5.2 Acclimation to temperature variations

Cell acclimate to temperature by adjusting the biosynthesis of key components (Hall et al. 2010; Ras et al. 2013). For example, Geider (1987) showed that phytoplankton cells are able to adapt their pigment content when temperature changes. The chlorophyll concentration is adjusted to the photon flux and to the cells capacity of converting it into chemical energy. The carbon to chlorophyll ratio ($\theta = Chl_a : C$) increases with temperature, and, following Geider (1987), this ratio converges after an acclimation phase to $\theta^*(T)$:

$$\theta^*(T) = \frac{e^{kT}}{(a - bT)e^{kT} + cI} \tag{42}$$

where $a, b, c, k$ are constants and $I$ is the light intensity. However, Eq. 42 is valid for balanced growth.

Dynamical models accounting for acclimation should therefore consider the different cellular components, and include the temperature effect on each reaction kinetic. Models for phytoplankton including chlorophyll have been proposed for example by Geider et al. (1998), but the temperature effect has been overlooked (assuming that all the kinetics have the same temperature dependence).

In Bernard et al. (2015), an equation for cell acclimation is proposed, which can be straightforwardly extended to acclimation to temperature:

$$\dot{\theta} = \delta\, \mu(T)\, [\theta^*(T) - \theta] \tag{43}$$

where $\delta$ is a parameter modulating the acclimation rate, which is assumed proportional to the growth rate $\mu$. This kind of models is of particular interest given that it can deal with both temperature fluctuations and the interplay with other factors such as light, but more experimental data are required for calibration and validation.

## 6 Conclusion and future developments

To better picture the temperature effect, there is an urgent need for standard protocols, as proposed by Boyd et al. (2013), fulfilling two crucial points: (1) assess the growth rate with biomass proxies which are not influenced by temperature; (2) consider acclimation periods of at least one week for each temperature. Such a protocol is required to isolate the impact of temperature on growth and to compare different experimental results.

Despite their simplicity, empirical models turn out to be very acute for representing the experimental data sets for phytoplankton (see Fig. 2). Nonetheless, to be efficient, these models must be associated to tailored calibration algorithms in line with Bernard and Rémond (2012) to rapidly fit a data set and quantify the uncertainty.

The mechanistic approach brings a complementary viewpoint in the modeling of the thermal growth curve but also in representing the temperature response for non-balanced growth conditions. Temperature plays a concurrent role on enzyme activity and therefore on reactions kinetics, and on cell structural stability. Most of the mechanistic models consider that a single enzyme controls growth at low temperatures (e.g. MMRM and proteome-scale approach) whereas temperature affects enzyme and protein conformational stability and leads to a decrease of growth at high temperatures (Ghosh et al. 2016). Despite the recent development of a promising unicellular growth model (Corkrey 2014), this 'proteome paradigm' should be further investigated for several reasons. First, the effect of temperature on protein stability is still relatively unclear given that we do not know, for example, in which extent proteins denaturation proceeds the same way in vivo as in vitro (Leuenberger et al. 2017). Second, other structural components play an important role in the cell thermal stability, and especially on membrane fluidity (Caspeta et al. 2014). Third, cells have the capacity to repair their damages and regrow after a heat shock (Li and Srivastava 2004) which is not clearly understood, as well as the molecular mechanisms protecting against mortality (Ghosh et al. 2016). Finally, the link between the mortality rate and protein denaturation still remains unclear; it is for example not known how mortality increases between $T_{opt}$ and $T_{max}$. Mortality models in line with Serra-Maia et al. (2016) are needed. In addition to the 'proteome paradigm' limits, the effect of temperature on cells kinetics is not limited to one enzyme controlling growth, but apply for all reactions. Some authors, for example, claim that the thermal

growth curve is the result of an imbalance of cellular energy allocation (called the metabolic hypothesis; Ruoff et al. 2007; Poertner 2012; Zakhartsev et al. 2015). The use of metabolic models under non-balanced growth should be used to challenge this problematic (Baroukh 2014). Additionally, models describing the dynamics of acclimation should be used to tackle the cellular response to temperature variations at different time-scales (Ras et al. 2013).

This work is a step towards the comprehension of the effect of global warming on phytoplankton. To do so, new thermal models should be designed to represent the temperature coupling with the most important growth factors. For phytoplankton, some models accounting for light and temperature have been validated on experimental data (Bernard and Rémond 2012), but we do not know in which extent they can be used. For example, the effect of temperature at high light intensity has not clearly been investigated. The development of cell-scaled models representing the different states of the photosystem centers and their temperature sensitivities [as done, for example, by Duarte (1995)] should help to better understand the temperature and light coupling. For nutrients, the coupling effect of temperature and starvation have a drastic impact on growth, and models are in development (Thomas 2013; Thomas et al. 2017).

It is worth noting that we did not describe adaptation models at the evolutionary time-scale which are needed to understand long time effects of an increase in temperature on the thermal response. These models, mostly based on the adaptive dynamics theory, are currently being developed (Thomas 2013; Grimaud 2016) and should be the next stage to understand the effect of global warming on oceans.

**Acknowledgements** This work was supported by the ANR Purple Sun Project ANR-13-BIME-004. We are grateful to Quentin Béchet, Colin Kremer, Mridul Thomas and the Litchman&Klausmeier Lab for their interesting comments on the paper. We also thank the three anonymous reviewers for their helpful suggestions.

## References

Akaike H (1992) Information theory and an extension of the maximum likelihood principle. In: Breakthroughs in statistics. Springer, New York, pp 610–624

Arrhenius S (1889) On the reaction velocity of the inversion of cane sugar by acids. Zeitschrift für Physikalische Chemie 4:226–248

Augustin JC, Carlier V (2000) Modelling the growth rate of listeria monocytogenes with a multiplicative type model including interactions between environmental factors. Int J Food Microbiol 56(1):53–70

Baranyi J, Roberts TA (1995) Mathematics of predictive food microbiology. Int J Food Microbiol 26(2):199–218

Baranyi J, Robinson T, Kaloti A, Mackey B (1995) Predicting growth of brochothrix thermosphacta at changing temperature. Int J Food Microbiol 27(1):61–75

Baroukh C (2014) Metabolic modeling under non-balanced growth. Application to microalgae for biofuels production. PhD thesis, Université Montpellier 2

Bernard O, Rémond B (2012) Validation of a simple model accounting for light and temperature effect on microalgal growth. Bioresour Technol 123:520–527

Bernard O, Mairet F, Chachuat B (2015) Modelling of microalgae culture systems with applications to control and optimization. In: Microalgae biotechnology. Springer International Publishing, pp 59–87

Bischof JC, He X (2005) Thermal stability of proteins. N Y Acad Sci 1066:12–33

Blanchard GF, Guarini JM, Richard P, Gros P, Mornet F (1996) Quantifying the short-term temperature effect on light-saturated photosynthesis of intertidal microphytobenthos. Mar Ecol Prog Ser 134:309–313

Boyd PW, Rynearson TA, Armstrong EA, Fu F, Hayashi K, Hu Z, Hutchins DA, Kudela RM, Litchman E, Mulholland MR, Passow U, Strzepek RF, Whittaker KA, Yu E, Thomas MK (2013) Marine phytoplankton temperature versus growth responses from polar to tropical waters outcome of a scientific community-wide study. PLoS ONE 8:e63,091. doi:10.1371/journal.pone.0063091

Brauer V, Stomp M, Rosso C, van Beusekom S, Emmerich B, Stal L, Huisman J (2013) Low temperature delays timing and enhances the cost of nitrogen fixation in the unicellular cyanobacterium cyanothece. ISME J 13:1–11

Campbell A (1957) Synchronization of cell division. Bacteriol Rev 21(4):263

Caspeta L, Chen Y, Ghiaci P, Feizi A, Buskov S, Hallström BM, Petranovic D, Nielsen J (2014) Altered sterol composition renders yeast thermotolerant. Science 346(6205):75–78

Chen P, Shakhnovich EI (2010) Thermal adaptation of viruses and bacteria. Biophys J 98(7):1109–1118

Corkrey R, McMeekin TA, Bowman JP, Ratkowsky DA, Olley J, Ross T (2014) Protein thermodynamics can be predicted directly from biological growth rates. PloS ONE 9(5):e96,100

Corradini MG, Peleg M (2006) On modeling and simulating transitions between microbial growth and inactivation or vice versa. Int J Food Microbiol 108(1):22–35

Danson MJ, Hough DW, Russell RJ, Taylor GL, Pearl L (1996) Enzyme thermostability and thermoactivity. Protein Eng 9(8):629–630

Dermoun D, Chaumont D, Thebault JM, Dauta A (1992) Modelling of growth of porphyridium cruentum in connection with two interdependent factors: light and temperature. Bioresour Technol 42(2):113–117

Dill KA, Ghosh K, Schmit JD (2011) Physical limits of cells and proteomes. Proc Natl Acad Sci 108(44):17,876–17,882
Droop M (1968) Vitamin B12 and marine ecology. IV. The kinetics of uptake, growth and inhibition in monochrysis lutheri. J Mar Biol Assoc UK 48(3):689–733
Duarte P (1995) A mechanistic model of the effects of light and temperature on algal primary productivity. Ecol Model 82(2):151–160
Edwards KF, Thomas MK, Klausmeier CA, Litchman E (2016) Phytoplankton growth and the interaction of light and temperature: a synthesis at the species and community level. Limnology and Oceanography. doi:10.1002/lno.10282
Eijsink VG, Gåseidnes S, Borchert TV, van den Burg B (2005) Directed evolution of enzyme stability. Biomol Eng 22(1):21–30
Eppley RW (1972) Temperature and phytoplankton growth in the sea. Fish Bull 70:1063–1085
Eyring H (1935) The activated complex in chemical reactions. J Chem Phys 3(2):107–115
Falkowski PG, Raven JA (2013) Aquatic photosynthesis. Princeton University Press, Princeton
Field CB, Behrenfled MJ, Randerson JT, Falkowski PG (1998) Primary production of the biosphere: integrating terrestrial and oceanic components. Science 281:237
Follows MJ, Dutkiewicz S, Grant S, Chisholm SW (2007) Emergent biogeography of microbial communities in a model ocean. Science 315(5820):1843–1846
Frauenfelder H, Sligar SG, Wolynes PG (1991) The energy landscapes and motions of proteins. Science 254(5038): 1598–1603
Frey SD, Lee J, Melillo JM, Six J (2013) The temperature response of soil microbial efficiency and its feedback to climate. Nat Clim Change 3(4):395–398
Fuhrman JA, Cram JA, Needham DM (2015) Marine microbial community dynamics and their ecological interpretation. Nat Rev Microbiol 13(3):133–146
Geider R (1987) Light and temperature dependence of the carbon to chlorophyll a ratio in microalgae and cyanobacteria: implications for physiology and growth of phytoplankton. New Phytol 106(1):1–34
Geider RJ, MacIntyre KL, Kana TM (1998) A dynamic regulatory model of phytoplanktonic acclimation to light, nutrients, and temperature. Limnol Oceanogr 43:679–694
Ghosh K, Dill K (2010) Cellular proteomes have broad distributions of protein stability. Biophys J 99(12):3996–4002
Ghosh K, de Graff AM, Sawle L, Dill KA (2016) Role of proteome physical chemistry in cell behavior. J Phys Chem B 120(36):9549–9563
Gillooly JF, Brown JH, West GB, Savage VM, Charnov EL (2001) Effects of size and temperature on metabolic rate. Science 293(5538):2248–2251
Grimaud GM (2016) Modelling the effect of temperature on phytoplankton growth: from acclimation to adaptation. PhD thesis, Université de Nice-Sophia Antipolis
Hall EK, Singer GA, Kainz MJ, Lennon JT (2010) Evidence for a temperature acclimation mechanism in bacteria: an empirical test of a membrane-mediated trade-off. Funct Ecol 24(4):898–908
Hinshelwood CN (1945) The chemical kinetics of bacterial cells. Clarendon Press, Oxford
Hobbs JK, Jiao W, Easter AD, Parker EJ, Schipper LA, Arcus LV (2013) Change in heat capacity for enzyme catalysis determines temperature dependence of enzyme catalyzed rates. ACS Chem Biol 8:2388–2393
Holcomb DL, Smith MA, Ware GO, Hung YC, Brackett RE, Doyle MP (1999) Comparison of six dose-response models for use with food-borne pathogens. Risk Anal 19(6):1091–1100
Jensen S, Knutsen G (1993) Influence of light and temperature on photoinhibition of photosynthesis inspirulina platensis. J Appl Phycol 5(5):495–504
Johnson FH, Lewin I (1946) The growth rate of *E. coli* in relation to temperature, quinine and coenzyme. J Cell Comp Physiol 28(1):47–75
Kingsolver JG (2009) The well-temperatured biologist. Am Nat 174:755–768
Kooijman SALM (2010) Dynamic energy budget theory for metabolic organisation. Cambridge University, Cambridge
Leuenberger P, Ganscha S, Kahraman A, Cappelletti V, Boersema PJ, von Mering C, Claassen M, Picotti P (2017) Cell-wide analysis of protein thermal unfolding reveals determinants of thermostability. Science 355(6327):eaai7825
Li Z, Srivastava P (2004) Heat-shock proteins. Curr Protoc Immunol A–1T. doi:10.1002/0471142735.ima01ts58
Lloyd J, Taylor J (1994) On the temperature dependence of soil respiration. Funct Ecol 315–323.
Lobry JR, Rosso L, Flandrois JP (1991) A fortran subroutine for the determination of parameter confidence limits in non-linear models. Binary 3:86–93
Mafart P, Couvert O, Gaillard S, Leguérinel I (2002) On calculating sterility in thermal preservation methods: application of the Weibull frequency distribution model. Int J Food Microbiol 72(1):107–113
Moats WA (1971) Kinetics of thermal death of bacteria. J Bacteriol 105(1):165–171
Murphy KP, Gill SJ (1991) Solid model compounds and the thermodynamics of protein unfolding. J Mol Biol 222(3):699–709
Murphy KP, Privalov PL, Gill SJ (1990) Common features of protein unfolding and dissolution of hydrophobic compounds. Science 247(4942):559–561
Norberg J (2004) Biodiversity and ecosystem functioning: a complex adaptive systems approach. Limnol Oceanogr 49:1269–1277
Paul EA (2014) Soil microbiology, ecology and biochemistry. Academic Press, Cambridge
Peeters J, Eilers P (1978) The relationship between light intensity and photosynthesis—a simple mathematical model. Hydrobiol Bull 12(2):134–136
Pena MI, Davlieva M, Bennett MR, Olson JS, Shamoo Y (2010) Evolutionary fates within a microbial population highlight an essential role for protein folding during natural selection. Mol Syst Biol 6(1):387
Pittera J, Humily F, Thorel M, Grulois D, Garczarek L, Six C (2014) Connecting thermal physiology and latitudinal niche partitioning in marine synechococcus. ISME J 118:1751–7370
Poertner HO (2012) Integrating climate-related stressor effects on marine organisms: unifying principles linking molecule to ecosystem-level changes. Mar Ecol Prog Ser 470:273–290

Pomeroy LR, Wiebe WJ (2001) Temperature and substrates as interactive limiting factors for marine heterotrophic bacteria. Aquat Microb Ecol 23(2):187–204
Privalov P, Khechinashvili N (1974) A thermodynamic approach to the problem of stabilization of globular protein structure: a calorimetric study. J Mol Biol 86(3):665–684
Privalov PL (1979) Stability of proteins small globular proteins. Adv Protein Chem 33:167–241
Ras M, Steyer JP, Bernard O (2013) Temperature effect on microalgae: a crucial factor for outdoor production. Rev Environ Sci Bio/Technol 12(2):153–164
Ratkowksy D, Lowry R, McMeekin T, Stokes A, Chandler R (1983) Model for bacterial culture growth rate throughout the entire biokinetic temperature range. J Bacteriol 154:1222–1226
Ratkowsky D, Olley J, McMeekin TA, Ball A (1982) Relationship between temperature and growth rate of bacterial cultures. J Bacteriol 149(1):1–5
Ratkowsky DA, Olley J, Ross T (2005) Unifying temperature effects on the growth rate of bacteria and the stability of globular proteins. J Theor Biol 233(3):351–362
Robertson AD, Murphy KP (1997) Protein structure and the energetics of protein stability. Chem Rev 97(5):1251–1268
Rogelj J, Meinshausen M, Knutti R (2012) Global warming under old and new scenarios using IPCC climate sensitivity range estimates. Nat Clim Change 2(4):248–253
Rosenberg B, Kemeny G, Switzer RC, Hamilton TC (1971) Quantitative evidence for protein denaturation as the cause of thermal death. Nature 232:471–473
Ross T (1993) A philosophy for the development of kinetic models in predictive microbiology. PhD thesis, University of Tasmania
Rosso L, Lobry J, Flandrois J (1993) An unexpected correlation between cardinal temperatures of microbial growth highlighted by a new model. J Theor Biol 162:447–463
Ruoff P, Zakhartsev M, Westerhoff HV (2007) Temperature compensation through systems biology. FEBS J 274(4):940–950
Sawle L, Ghosh K (2011) How do thermophilic proteins and proteomes withstand high temperature? Biophys J 101(1):217–227
Schipper LA, Hobbs JK, Ruledge S, Arcus VL (2014) Thermodynamic theory explains the temperature optima of soil microbial processes and high Q10 values at low temperatures. Glob Change Biol 20:3578–3586
Schwarz G et al (1978) Estimating the dimension of a model. Ann Stat 6(2):461–464
Serra-Maia R, Bernard O, Gonçalves A, Bensalem S, Lopes F (2016) Influence of temperature on chlorella vulgaris growth and mortality rates in a photobioreactor. Algal Res 18:352–359
Slator A (1916) II. The rate of growth of bacteria. J Chem Soc Trans 109:2–10
Smelt J, Brul S (2014) Thermal inactivation of microorganisms. Crit Rev Food Sci Nutr 54(10):1371–1385
Smelt JP, Hellemons JC, Wouters PC, van Gerwen SJ (2002) Physiological and mathematical aspects in setting criteria for decontamination of foods by physical means. Int J Food Microbiol 78(1):57–77
Snyder CD (1906) The influence of temperature upon the rate of heart beat in the light of the law for chemical reaction velocity. II. Am J Physiol Leg Content 17(4):350–361
Song Y, Chen Q, Ci D, Shao X, Zhang D (2014) Effects of high temperature on photosynthesis and related gene expression in poplar. BMC Plant Biol 14(1):111
Taucher J, Jones J, James A, Brzezinski MA, Carlson CA, Riebesell U, Passow U (2015) Combined effects of $CO_2$ and temperature on carbon uptake and partitioning by the marine diatoms *Thalassiosira weissflogii* and *Dactyliosolen fragilissimus*. Limnol Oceanogr 60(3):901–919
Thomas M (2013) The effect of temperature on the ecology, evolution, and biogeography of phytoplankton. PhD thesis, Michigan State University
Thomas M, Kremer C, Klausmeier C, Litchman E (2012) A global pattern of thermal adaptation in marine phytoplankton. Science 338:1085–1088
Thomas MK, Litchman E (2016) Effects of temperature and nitrogen availability on the growth of invasive and native cyanobacteria. Hydrobiologia 763(1):357–369
Thomas MK, Aranguren-Gassis M, Kremer CT, Gould MR, Anderson K, Klausmeier CA, Litchman E (2017) Temperature–nutrient interactions exacerbate sensitivity to warming in phytoplankton. Glob Change Biol. doi:10.1111/gcb.13641
Valik L, Medvedova A, Cizniar M, Liptakova D (2013) Evaluation of temperature effect on growth rate of lactobacillus rhamnosus GG in milk using secondary models. Chem Pap 67(7):737–742
van Gestel NC, Reischke S, Bååth E (2013) Temperature sensitivity of bacterial growth in a hot desert soil with large temperature fluctuations. Soil Biol Biochem 65:180–185
Van Uden N (1985) Temperature profiles of yeasts. Adv Microb Physiol 25:195–251
Vezzulli L, Brettar I, Pezzati E, Reid PC, Colwell RR, Höfle MG, Pruzzo C (2012) Long-term effects of ocean warming on the prokaryotic community: evidence from the vibrios. ISME J 6(1):21–30
Young JN, Goldman JA, Kranz SA, Tortell PD, Morel FM (2015) Slow carboxylation of rubisco constrains the rate of carbon fixation during antarctic phytoplankton blooms. New Phytol 205(1):172–181
Zakhartsev M, Yang X, Reuss M, Pörtner HO (2015) Metabolic efficiency in yeast saccharomyces cerevisiae in relation to temperature dependent growth and biomass yield. J Therm Biol 52:117–129
Zeldovich KB, Chen P, Shakhnovich EI (2007) Protein stability imposes limits on organism complexity and speed of molecular evolution. Proc Natl Acad Sci 104(41):16,152–16,157
Zhang J (2000) Protein-length distributions for the three domains of life. Genome Anal 16(3):107–109
Zwietering MH, Wijtzes T, Rombouts FM, van't Riet K (1993) A decision support system for prediction of microbial spoilage in foods. J Ind Microbiol 12(3–5):324–329